Scanning tunneling microscopy evidence for the Mars-van Krevelen type mechanism of low temperature CO oxidation on an FeO(1 1 1) film on Pt(1 1 1)

M. Lewandowski, I.M.N. Groot, S. Shaikhutdinov *, H.-J. Freund

Abteilung Chemische Physik, Fritz-Haber-Institut der Max-Planck-Gesellschaft, Faradayweg 4-6, 14195 Berlin, Germany

A B S T R A C T

We provide experimental evidence that the low temperature CO oxidation reaction on an ultrathin FeO(1 1 1) film on Pt(1 1 1) proceeds through the Mars-van Krevelen type mechanism which includes the following steps: the FeO film is oxidized into an FeO_{2-x} film with trilayer O–Fe–O structure; CO reacts with the weakly bound, topmost oxygen atoms, effectively reducing the FeO_{2-x} surface to FeO-like; and the subsequent oxidation by O_2 recovers the FeO_{2-x} structure.

© 2011 Elsevier B.V. All rights reserved.

1. Introduction

The catalytic oxidation of CO over platinum group metals is one of the most widely studied reactions in heterogeneous catalysis (e.g., see reviews [1–3] and references therein). Due to its technological importance in automotive catalysts [4] and fuel cells [5,6], detailed studies have been performed on model systems, primarily on Pt(1 1 1) single crystals, to unravel the reaction mechanisms. It is now well established that the oxidation reaction follows the Langmuir–Hinshelwood mechanism, in which CO_2 is formed through the associative reaction of chemisorbed CO and O atoms dissociatively adsorbed on the surface [1]. Note that the CO oxidation reaction on platinum surfaces may even show oscillatory behavior, which was observed on Pt(1 1 1) only at relatively high pressures as the reaction proceeds most likely through surface oxidation–reduction cycles [7].

Recently, it has been found that thin oxide films grown on metals can promote this reaction at low temperatures [8,9]. Indeed, a monolayer film of FeO(1 1 1) grown on Pt(1 1 1) showed activity for CO oxidation already at 450 K, i.e., at a temperature where bare Pt(1 1 1) is almost inactive [8]. The concept of using thin films as catalysts was further demonstrated on supported systems where metal nanoparticles were encapsulated by a thin oxide film as a result of strong metal-support interaction with a reducible support [10–12]. Also, for a three monolayer thick MgO film on Ag(1 0 0), a density functional theory (DFT) study predicted CO oxidation with a much lower activation barrier than on Pt(1 1 1) [9] (experimentally not proven yet).

The atomic structure of ultrathin FeO(1 1 1) films on Pt(1 1 1) is well documented in the literature [13]. It consists of close-packed layers of Fe and O, stacked as O–Fe–Pt, and exhibits a Moiré pattern due to the lattice mismatch between the FeO(1 1 1) and Pt(1 1 1) lattices. However, it has been found that, at elevated oxygen pressures, the bilayer O–Fe film transforms into a trilayer O–Fe–O film [8,14]. This reaction is computed to be site specific within the large (ca. 2.6 nm) Moiré unit cell [15], that may explain scanning tunneling microscopy (STM) results showing the formation of close-packed FeO_2 islands rather than a continuous FeO_2 film [14]. In addition, it has been shown that the FeO_2 islands exhibit $(\sqrt{3} \times \sqrt{3})R30°$ reconstruction which has tentatively been assigned to the relaxation of the Fe layer between the O-layers.

The reaction mechanism of CO oxidation on the O-rich films was addressed by DFT using the model of a continuous FeO_2 film [14,15]. It was proposed that the reaction follows the Mars-van Krevelen (M-vK) type mechanism where CO reacts with the weakly bound, topmost oxygen atom of an FeO_2 film and forms CO_2 that desorbs leaving an oxygen vacancy behind. This vacancy must be replenished by the reaction with molecular oxygen to end the catalytic cycle. A comparative study with NO as an oxidative agent led to the conclusion that the replenishment of oxygen vacancies is the rate-limiting step [16].

In principle, the complex structure of the FeO_{2-x} film may suggest various sites for this reaction, i.e., not only regular sites on top of the FeO_2 islands computed in the DFT studies, but also yet ill-defined structures between the FeO_2 islands as well as other defects. In addition, in the case of ultrathin films on metals, reaction mechanisms including activation of adsorbates by electron transfer

* Corresponding author.
  E-mail address: shaikhutdinov@fhi-berlin.mpg.de (S. Shaikhutdinov).

from the oxide/metal interface cannot be ruled out [17–22], albeit the very high work function of FeO/Pt(1 1 1) renders this process unlikely.

In continuation of our previous work, here we report experimental results showing that the reaction proceeds through the Mars-van Krevelen mechanism on the FeO_{2-x} films, i.e., cycles of surface reduction by CO and oxidation of the reduced surface with O_2.

2. Experimental

The experiments were performed in an ultra-high vacuum (UHV) chamber equipped with Auger electron spectroscopy (AES), low energy electron diffraction (LEED), a quadrupole mass spectrometer, and STM. In addition, a high-pressure (HP) cell is connected to the main UHV chamber through a gate valve. The Pt(1 1 1) sample is mounted to a Pt sample holder to prevent contamination by any volatile species formed at high pressures. The temperature is measured using a chromel-alumel thermocouple spot welded to the edge of the crystal. In the UHV chamber, the sample can be heated by electron bombardment from the backside using a tungsten filament. In the HP cell, the crystal is heated from the backside using a halogen lamp.

The Pt(1 1 1) crystal was cleaned using repeated cycles of Ar^+ bombardment, followed by oxidation in 3×10^{-6} mbar O_2 at 1000 K and subsequent annealing in UHV at 1200 K. Morphology and cleanliness of the crystal were checked by LEED, STM and AES prior to each preparation of the FeO(1 1 1) film that includes the vapor deposition of one monolayer of Fe (Goodfellow, 99.95%) onto the clean Pt(1 1 1) surface at room temperature, and subsequent oxidation in 1×10^{-6} mbar O_2 at 1000 K for 2 min.

For the HP treatments, CO (99.995%) and O_2 (99.999%) were introduced into the cell through a cold trap kept at ~150 K. After each treatment, the sample was cooled down to room temperature while the cell was pumped out down to ~10^{-6} mbar before it was transferred back to the main UHV chamber for surface characterization.

3. Results and discussion

The previous results showed that the first step in making the FeO(1 1 1)/Pt(1 1 1) film active is its transformation into the O-rich, FeO_{2-x} film that occurs only in the mbar range of oxygen pressure. In contrast, exposure to CO does not chemically reduce or considerably modify the FeO(1 1 1) film surface at the same pressure and temperature. If the CO oxidation reaction in the mixture of CO and O_2 proceeds primarily through the activation of adsorbed species at the surface, then the FeO_{2-x} film would maintain its surface structure upon exposure to CO, as the oxygen atoms in the film (i.e., lattice oxygen) are not involved in the reaction. In contrast, following the M-vK mechanism the oxide surface will effectively be reduced in the CO-rich ambient. In this case, the active sites for the reaction could be titrated by CO and (if so) be imaged, for example, by STM. Following this idea, we performed structural characterization of the FeO films sequentially treated with pure O_2 and CO.

Fig. 1a shows an STM image of an FeO/Pt(1 1 1) film exposed to 50 mbar O_2 at 450 K for 10 min. In full agreement with our previous work, the FeO(1 1 1) film is completely transformed into the O-rich film of compositional stoichiometry FeO_{2-x} ($x \sim 0.1$), as measured by AES (Fig. 2). The film exhibits long-range ordering similar to the Moiré structure of the original FeO(1 1 1) film as judged by the LEED pattern shown below the image in Fig. 1a. The periodic ~3 nm wide protrusions in this image correspond to the FeO_2 islands of similar size as the Moiré unit cell. The close-packed domains of FeO_2 islands within the same terrace are often slightly rotated with respect to each other [15].
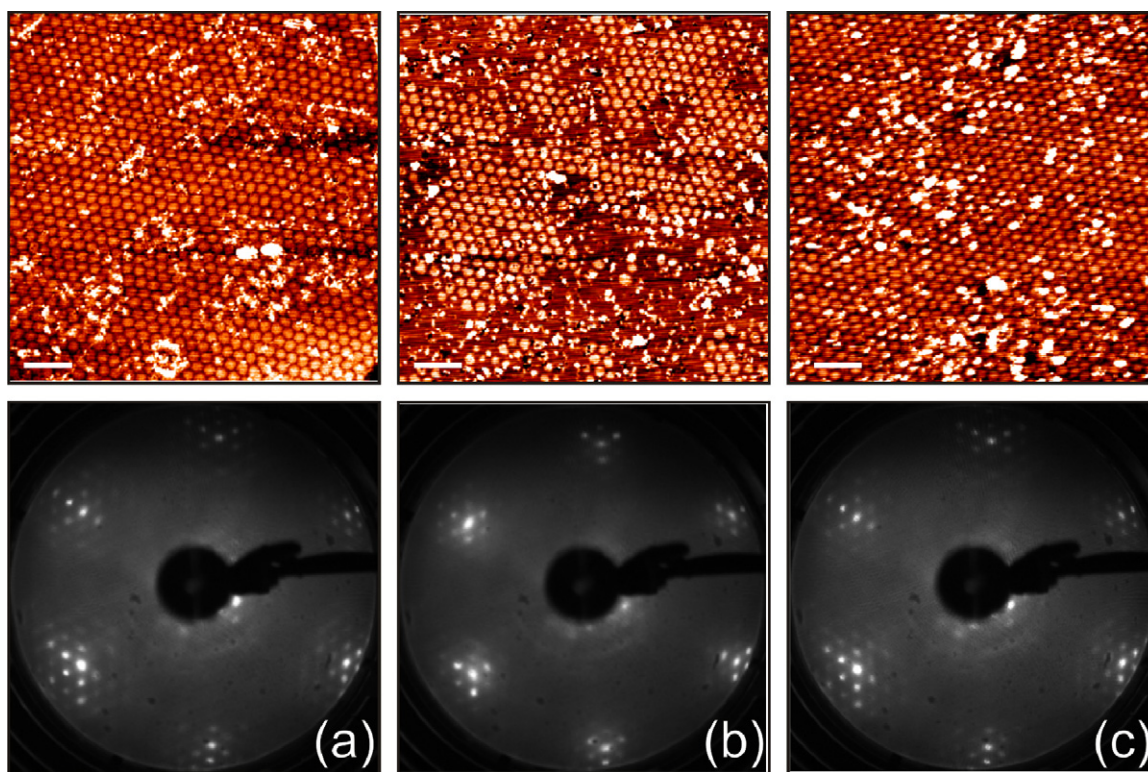

Fig. 1. STM images (top panel) and LEED patterns (bottom panel) of an FeO(1 1 1)/Pt(1 1 1) film after sequential exposure to 50 mbar O_2 at 450 K for 10 min (a), 10 mbar CO at 450 K for 10 min (b), and again to 50 mbar O_2 at 450 K for 10 min (c). Images are obtained at room temperature in vacuum. The scale bar corresponds to 10 nm. Sample bias 1.0 V (a and b) and 1.4 V (c), tunneling current 0.7 nA.
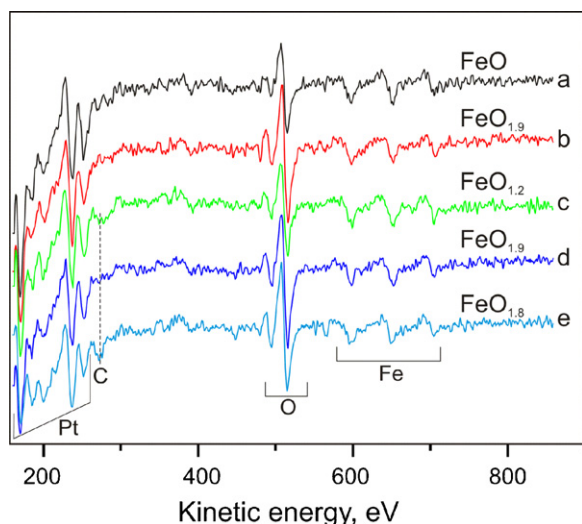
Fig. 2. Auger spectra of an FeO(1 1 1) film (a) subsequently oxidized in 50 mbar of O_2 at 450 K for 10 min (b); then exposed to 10 mbar CO at 450 K for 10 min (c); and finally to 50 mbar of O_2 at 450 K for 10 min (d) (see the corresponding STM images in Fig. 1). Spectrum (e) is obtained after an FeO film was exposed to 10 mbar of O_2 at 700 K for 10 min (see STM image in Fig. 3). The compositional stoichiometry derived from the spectra using FeO as the reference are indicated.

Oxidation at higher temperature, i.e., 700 K, does not considerably alter the general morphology and stoichiometry of the film obtained at 450 K, except the formation of protruding worm-like features (see STM results in Fig. 3 and AES spectrum in Fig. 2). This finding suggests that the formation of FeO_2 islands rather than a continuous FeO_2 film is thermodynamically driven. The randomly distributed protruding spots in Fig. 1a (~3 Å in height), which apparently aggregate into protruding lines seen in Fig. 2, can be assigned to carbon contaminations detected by AES (see Fig. 2). Another option would be ill-defined FeO_x clusters formed in the course of the FeO → FeO_2 transformation, which is accompanied by small changes in the lattice parameter [15].
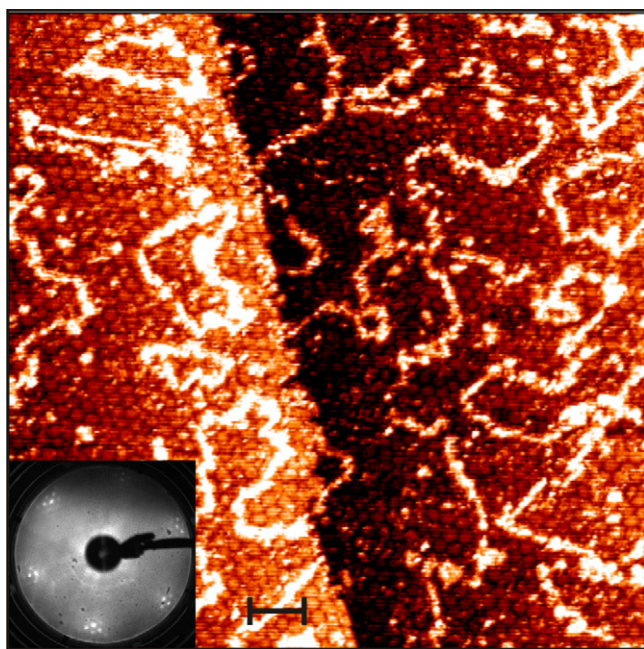

Fig. 3. STM image and LEED pattern of an FeO(1 1 1) film oxidized at 10 mbar O_2 at 700 K for 10 min. The scale bar corresponds to 10 nm. Sample bias 1.0 V, tunneling current 0.7 nA.

In the next step, the film was exposed to 10 mbar CO at 450 K. The reaction time was limited to 10 min in order to monitor the initial stages of structural transformation and also to preclude film dewetting that always occurs in a CO-rich atmosphere [8,23]. The long-range ordering of the film maintained during this treatment as judged by LEED (see the bottom panel in Fig. 1b). However, the O:Fe ratio has diminished from ~1.9 to ~1.2, as measured by AES (see Fig. 2). This fact alone indicates already that the FeO_{2-x} films strongly interact with CO at high pressures and undergo substantial chemical reduction via the CO + O(lattice) → CO_2 reaction as the reduction step in the M-vK mechanism.

An STM study of the CO-treated films revealed relatively large patches where the FeO_2 islands are totally missing, as shown in Fig. 1b. Profile line analysis showed that the patches are ~0.9 Å below the top surface of the FeO_2 islands, on average. This value is close to ~0.7 Å, measured for the height difference between the bilayer O–Fe and trilayer O–Fe–O films and also for the Fe–O interlayer distance in the FeO(1 1 1) films [15]. Although high resolution on a large scale was very difficult to achieve on the reduced patches, they often showed a ~3 Å periodicity (not shown) as in the original FeO(1 1 1) films. All these findings suggest that the surface between the remaining FeO_{2-x} domains is FeO-like in nature. In addition, the reduced surface also exhibits randomly distributed depressed areas (black spots) of ~0.9 Å in depth. Following the same argument of Fe–O interlayer distances, these spots can be attributed to Pt and/or Pt–Fe "holes" formed in the oxide film as a result of the total reduction. The reduced patches cover ca. 65% of the whole surface, on average. Taking into account also fully reduced spots, this value is fairly consistent with the AES data showing the $FeO_{1.2}$ stoichiometry of the CO-treated film. The fact that the Moiré pattern is not observed on the FeO-like patches could be explained by its slight disordering at the reaction temperature used (450 K), that is much lower than the temperatures needed for the preparation of the well-ordered FeO(1 1 1) films (>900 K).

In the final step, the partially reduced film was treated again with 50 mbar O_2 at 450 K for 10 min. The AES spectrum revealed a film stoichiometry of $FeO_{1.9}$, i.e., the same as after the first oxidation treatment. The large-scale STM image, shown in Fig. 1c, is virtually identical to that shown in Fig. 1a for the oxidized film, and as such clearly indicates that the FeO_{2-x} surface is fully recovered upon re-oxidation.

Therefore, the STM results, combined with LEED and AES data, strongly suggest that CO oxidation on FeO(1 1 1) films proceeds through the Mars-van Krevelen type mechanism, which includes surface reduction (by CO) and oxidation (by O_2) of the FeO_{2-x} surface.

More detailed analysis of the STM images of the CO-treated films revealed some interesting features, which could shed more light on the active sites for the CO oxidation reaction. First, the large-scale images showed that reduction of the FeO_{2-x} film by CO occurs homogeneously on the macroscopic scale in the range of hundreds of nanometers (not shown). In particular, the areas close to the step edges did not show any difference in morphology as compared to the terraces. However, on the microscopic scale, the oxide reduction seems to occur non-homogeneously. Certainly, the film morphology observed by STM *ex situ* could be kinetically limited. Nonetheless, the observation of extended areas with almost unchanged FeO_{2-x} morphology (see Fig. 1b), implies the presence of active sites where the reduction proceeds faster than on the regular FeO_2 islands, otherwise one would expect uniform disappearance of the islands. Moreover, if the reaction would take place on top of an FeO_2 island within a single domain, such islands would probably show circular (torroid-like) morphology. Alternatively, if the reaction starts between the close-packed FeO_2 islands, then the islands would uniformly shrink, resulting in the same domain just with smaller islands. None of such structures were observed in STM. In
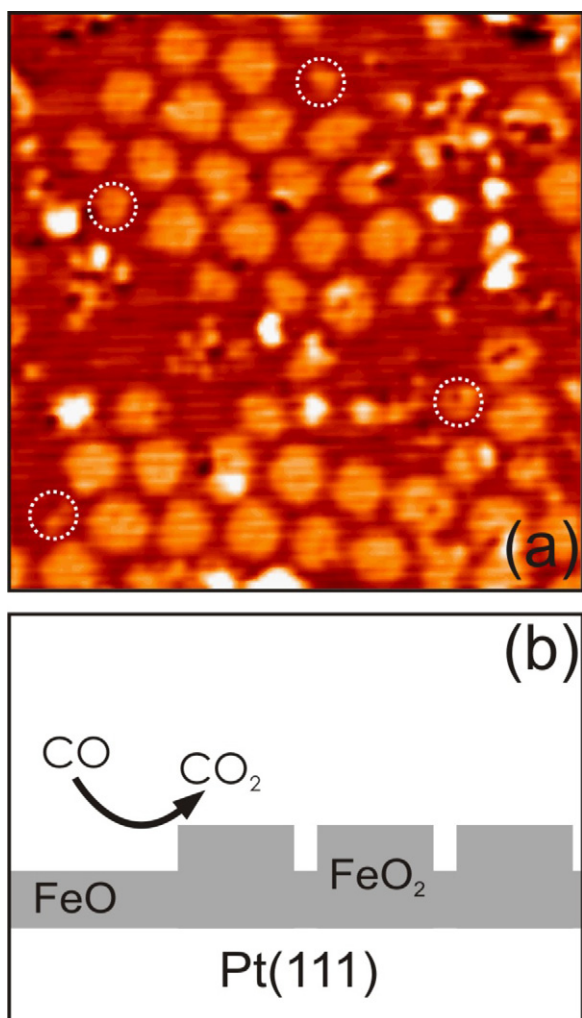
Fig. 4. (a) STM image (22 nm × 22 nm) of the CO-treated FeO_{2-x} films (see the large-scale image in Fig. 1b). Depressed (black) spots are assigned to the fully reduced surface. Some islands of smaller size observed at the border of the close-packed FeO_2 domains are marked in circles. (b) Schematic representation of the FeO_{2-x} film reduction by pure CO.

fact, the STM images revealed a majority of small islands at the border of the FeO_{2-x} domains, as shown in Fig. 4a. This suggests that the film reduction in the pure CO atmosphere occurs considerably faster at the interface between the reduced, FeO-like and the FeO_2 structures as schematically depicted in Fig. 4b. It appears that such sites, which are present in the oxidized films as defects, ignite the reduction process in pure CO ambient, which then propagates across the surface leaving the FeO-like surface behind. The origin of the defect sites responsible for the reaction ignition in these experiments is unclear. The oxidized, FeO_{2-x} surface is not so well ordered as the pristine FeO film and may, in principle, expose a variety of defects. It is unlikely, however, that the oxidized surface exposes the Pt (or Fe) metallic atoms since the temperature programmed desorption experiments did not show any CO adsorption on this surface at 100 K. Certainly, in situ spectroscopic techniques would help in elucidating the nature of the defect sites readily reacting with CO.

The complete back transformation of the O–Fe–O into the O–Fe film implies the Fe atoms migrating underneath the bottom O-layer upon removing the top O-layer by reaction with CO. However, the process can be (i) relatively slow at 450 K and (ii) affected by the presence of CO in the ambient, both effects stabilizing the Fe atoms

in the topmost layer. CO adsorbed on these Fe atoms can further react with oxygen in the film thus opening more Fe sites, or even leading to full reduction. This may explain why CO induced film dewetting, which opens the Pt(1 1 1) substrate, has been observed for the oxidized FeO_{2-x} films and not for the original, O-terminated FeO films [23]. Obviously, in the $CO + O_2$ mixture, the probability for such a scenario increases at the high CO/O_2 ratio, at which film dewetting has been observed [8,23]. Under the O_2-rich reaction conditions, oxidation of the Fe sites will prevent substantial reduction and result in the oxidized film structure.

4. Summary

We have performed a combined STM, LEED and AES study of FeO(1 1 1)/Pt(1 1 1) films sequentially exposed to pure O_2 and CO at pressures and temperatures used for the CO oxidation reaction over these films. Upon O_2 exposure the film transforms into the FeO_{2-x} film consisting of the close-packed FeO_2 islands as previously shown. Oxidation at elevated temperature (i.e., 700 K) does not considerably alter the general morphology of the film, thus suggesting that the formation of FeO_2 islands rather than a continuous FeO_2 film at high O_2 pressures is thermodynamically driven. Subsequent CO exposure effectively reduces the FeO_{2-x} surface to FeO-like via the CO reaction with the outermost oxygen atoms in the oxidized film. Re-oxidation by O_2 recovers the FeO_{2-x} structure. The results provide strong evidence that the CO oxidation reaction proceeds through the Mars-van Krevelen type mechanism.

References

[1] T. Engel, G. Ertl, Adv. Catal. 28 (1979) 1.
[2] P.J. Berlowitz, C.H.F. Peden, D.W. Goodman, J. Phys. Chem. 92 (1988) 5213.
[3] A.K. Santra, D.W. Goodman, Electrochim. Acta 47 (2002) 3595.
[4] J.T. Kummer, J. Phys. Chem. 90 (1986) 4747.
[5] J.N. Armor, Appl. Catal. A 176 (1999) 159.
[6] L. Carrette, K.A. Friedrich, U. Stimming, Fuel Cells 1 (2001) 5.
[7] R.E.R. Colen, J. Christoph, F. Pena, H.H. Rotermund, Surf. Sci. 408 (1998) 310.
[8] Y.N. Sun, Z.H. Qin, M. Lewandowski, E. Carrasco, M. Sterrer, S. Shaikhutdinov, H.-J. Freund, J. Catal. 266 (2009) 359.
[9] A. Hellman, S. Klacar, H. Gronbeck, J. Am. Chem. Soc. 131 (2009) 16636.
[10] Z.H. Qin, M. Lewandowski, Y.N. Sun, S. Shaikhutdinov, H.-J. Freund, J. Phys. Chem. C 112 (2008) 10209.
[11] Z.H. Qin, M. Lewandowski, Y.N. Sun, S. Shaikhutdinov, H.-J. Freund, J. Phys.: Condens. Matter 21 (2009) 134019.
[12] M. Lewandowski, Y.N. Sun, Z.H. Qin, S. Shaikhutdinov, H.-J. Freund, Appl. Catal. A 391 (2011) 407.
[13] W. Weiss, W. Ranke, Prog. Surf. Sci. 70 (2002) 1.
[14] Y.N. Sun, L. Giordano, J. Goniakowski, M. Lewandowski, Z.H. Qin, C. Noguera, S. Shaikhutdinov, G. Pacchioni, H.-J. Freund, Angew. Chem. Int. Ed. 49 (2010) 4418.
[15] L. Giordano, M. Lewandowski, I.M.N. Groot, Y.N. Sun, J. Goniakowski, C. Noguera, S. Shaikhutdinov, G. Pacchioni, H.-J. Freund, J. Phys. Chem. C 114 (2010) 21504.
[16] Y. Lei, M. Lewandowski, Y.N. Sun, Y. Fujimori, Y. Martynova, I.M.N. Groot, R. Meyer, L. Giordano, G. Pacchioni, J. Goniakowski, C. Noguera, S. Shaikhutdinov, H.-J. Freund, ChemCatChem 3 (4) (2011) 671–674.
[17] P. Frondelius, A. (0 () Hellman, K. Honkala, H. Hakkinen, H. Gronbeck, Phys. Rev. B 78 (2008) 085426.
[18] L. Giordano, G. Pacchioni, Phys. Chem. Chem. Phys. 8 (2006) 3335.
[19] G. Pacchioni, L. Giordano, M. Baistrocchi, Phys. Rev. Lett. 94 (2005).
[20] D. Ricci, A. Bongiorno, G. Pacchioni, U. Landman, Phys. Rev. Lett. 97 (2006).
[21] L. Giordano, G. Pacchioni, T. Risse, U.M. Pozzoni, L. Giordano, M. Heyde, H.P. Rust, G. Pacchioni, H.-J. Freund, Phys. Rev. Lett. 98 (2007).
[22] K. Honkala, H. Hakkinen, J. Phys. Chem. C 111 (2007) 4319.
[23] Y.N. Sun, Z.H. Qin, M. Lewandowski, S. Kaya, S. Shaikhutdinov, H.-J. Freund, Catal. Lett. 126 (2008) 31.